Reversible De-Intercalation and Intercalation Induced by Polymer Crystallization and Melting in a Poly(ethylene oxide)/Organoclay Nanocomposite

ARTICLE *in* LANGMUIR · JULY 2005

Impact Factor: 4.46 · DOI: 10.1021/la047087c · Source: PubMed

6 AUTHORS, INCLUDING:

Lei Zhu
Case Western Reserve University
162 PUBLICATIONS **3,923** CITATIONS
SEE PROFILE

Benjamin S Hsiao
Stony Brook University
571 PUBLICATIONS **20,574** CITATIONS
SEE PROFILE

Carlos A Avila-Orta
Centro de Investigación en Química Aplicada
71 PUBLICATIONS **1,109** CITATIONS
SEE PROFILE

Igors Sics
Cells Alba
73 PUBLICATIONS **2,360** CITATIONS
SEE PROFILE

Reversible De-Intercalation and Intercalation Induced by Polymer Crystallization and Melting in a Poly(ethylene oxide)/Organoclay Nanocomposite

Lu Sun,[†] Ethan A. Ertel,[†] Lei Zhu,*[,†] Benjamin S. Hsiao,[‡] Carlos A. Avila-Orta,[‡] and Igors Sics[‡]

Polymer Program, Institute of Materials Science and Department of Chemical Engineering, The University of Connecticut, Storrs, Connecticut 06269-3136, and Chemistry Department, State University of New York at Stony Brook, Stony Brook, New York 11794-3400

Received November 27, 2004. In Final Form: April 30, 2005

Semicrystalline polymer/layered silicate nanocomposites were prepared by solution blending of a low molecular weight poly(ethylene oxide) (PEO) with an organically modified montmorillonite, Cloisite 10A (C10A). The intercalation morphology was studied by temperature-dependent synchrotron wide-angle X-ray diffraction (WAXD). Unlike PEO homopolymers, significant secondary crystallization was observed in the PEO/C10A nanocomposites. Reversible de-intercalation and intercalation processes were detected during secondary crystallization and subsequent melting of secondary crystals. On the basis of two-dimensional WAXD results on oriented samples, an interphase layer between the silicate primary particles and PEO lamellar crystals was proposed. Secondary PEO crystallization in the interphase regions was inferred to be the primary driving force for polymer chains to diffuse out of the silicate gallery. This study provided a useful method to investigate polymer diffusion in nanoconfined spaces, which can be controlled by PEO secondary crystallization and melting outside the silicate gallery.

Introduction

Polymer/layered silicate nanocomposites are of substantial interest to both industry and academia because these materials (with only a few percent of loading of layered silicates) often exhibit unique properties which are different from conventional macro- or even microcomposites. For example, these properties include (1) improved mechanical properties in both modulus and tensile strength; (2) a remarkable increase in thermal stability as well as self-extinguishing characteristics for flammability; and (3) a several-fold reduction in the permeability of gases.[1−3] The drastic improvement in properties may be attributed to the large surface areas provided by the nanostructure of layered silicates. In addition, they can also serve as model systems to study chain conformation and dynamics in a confined space (or gallery) of 1-nm thickness.[4]

Stimulated by theoretical predictions of single-chain dynamics in confined geometries,[5] experiments have been carried out to deal with polymeric liquids confined at molecular length scales.[6−9] Depending on the nature of the polymer and the chemistry of the silicate surfaces, confinement can either reduce[6,7] or enhance[8,9] the local and global molecular dynamics. Among these studies, the melt intercalation of polymer chains into the nanometer scale galleries of layered silicates provided a useful tool to study the dynamics of nanoconfined polymer chains. The kinetics study of polystyrene (PS) melt-intercalation into organically modified fluorohectorite indicated that the hybrid formation was limited by mass transport from the bulk into the primary silicate particles and not specifically by diffusion of the polymers within the silicate galleries.[10] From wide-angle X-ray diffraction (WAXD) and small-angle neutron scattering experiments, the effective diffusion coefficient (D_{eff}) was obtained, which characterized the overall transport process of polymer chains from the bulk into the primary silicate particles and then into a confined environment.[11] The D_{eff} was found to be greater than the self-diffusion coefficient in an equilibrium melt, and the intercalation process was slower with increasing the affinity between polymer chains and silicate surfaces. Furthermore, the D_{eff} exhibited an inverse dependence on the chain length (N; $D_{eff} \propto N^{-1}$), as opposed to the equilibrium bulk self-diffusion coefficient scaling as N^{-2} in the reptation theory. These experimental findings were consistent with molecular dynamics simulations.[12,13]

In the hybrid composite environments, the local and global dynamics were found to be different from those in the bulk; especially on a local scale, the polymer chains exhibited higher flexibility with a suppression of cooperative motion associated with the glass transition.[14] In other words, the nanoconfined polymer chains exhibited liquid-like mobility even below the bulk glass transition temperature (T_g).[9] Two relaxation modes were observed for polymer chains confined in clay galleries using surface-sensitive cross-polarization with spin−echo nuclear magnetic resonance (NMR) measurements[9] and dielectric

* Corresponding author. E-mail: lei.zhu@uconn.edu.
[†] The University of Connecticut.
[‡] State University of New York at Stony Brook.

(1) Ray, S. S.; Okamoto, M. *Prog. Polym. Sci.* **2003**, *28*, 1539.
(2) Fischer, H. *Mater. Sci. Eng. C* **2003**, *23*, 763.
(3) Schmidt, D.; Shah, D.; Giannelis, E. P. *Curr. Opin. Solid State Mater. Sci.* **2002**, *6*, 205.
(4) Giannelis, E. P. *Adv. Mater.* **1996**, *8*, 29.
(5) de Gennes, P.-G. *Scaling Concepts in Polymer Physics*; Cornell University Press: Ithaca, NY, 1979.
(6) Demirel, A.; Granick, S. *Phys. Rev. Lett.* **1996**, *77*, 2261.
(7) Jerome, B.; Commandeur, J. *Nature* **1997**, *386*, 589.
(8) Anastasiadis, S. H.; Karatasos, K.; Vlachos, G.; Manias, E.; Giannelis, E. P. *Phys. Rev. Lett.* **2000**, *84*, 915.
(9) Zax, D. B.; Yang, D.-K.; Santos, R. A.; Hegemann, H.; Giannelis, E. P.; Manias, E. *J. Chem. Phys.* **2000**, *112*, 2945.
(10) Vaia, R. A.; Jandt, K. D.; Kramer, E. J.; Giannelis, E. P. *Macromolecules* **1995**, *28*, 8080.
(11) Manias, E.; Chen, H.; Krishnamoorti, R.; Genzer, J.; Kramer, E. J.; Giannelis, E. P. *Macromolecules* **2000**, *33*, 7955.
(12) Lee, J. Y.; Baljon, A. R. C.; Loring, R. F. *J. Chem. Phys.* **1999**, *111*, 9754.
(13) Lee, J. Y.; Loring, R. F. *Macromolecules* **2001**, *34*, 5727.
(14) Krishnamoorti, R.; Vaia, R. A.; Giannelis, E. P. *Chem. Mater.* **1996**, *8*, 1728.

10.1021/la047087c CCC: $30.25
Published on Web 05/18/2005

relaxation spectroscopy.[8] Polymers in the center of the gallery were more mobile than those in the bulk at the same temperatures, while chain segments interacting with the silicate surface were dynamically inhibited. Computer simulation of the molecular details at the interfaces provided more insights and confirmed these heterogeneities of the polymer chains confined in nanospaces.[15,16] The confined polymer chains also exhibited unusual conformations as studied by NMR techniques. For example, the OC−CO bonds of poly(ethylene oxide) (PEO) chains confined in <1.0-nm gaps exhibited a high gauche content of about 90%, which was much higher than that in amorphous bulk PEO (25%) and also different from the cases in certain complexes of PEO with $HgCl_2$ ($TGGT\bar{G}\bar{G}$).[17] Different chain conformations were believed to affect the chain diffusion property in confined spaces.

In the present study, we explored a novel route to investigate chain diffusion within a nanoconfined slab, which could eliminate the diffusion process of PEO chains from the bulk into the primary silicate particles in melt intercalation experiments, as mentioned above.[10] A low molecular weight PEO was solution blended with an organically modified natural montmorillonite, Cloisite 10A (C10A), using chloroform as the solvent. The PEO intercalated in the C10A galleries was amorphous in the entire temperature range studied, while the rest PEO outside the C10A tactoids was crystallizable. Reversible de-intercalation and intercalation were observed in response to PEO secondary crystallization and subsequent melting of secondary crystals. The self-generated depletion field by the PEO crystallization in the interphase regions between silicate particles and PEO primary lamellar crystals is speculated to be the driving force for the intercalated PEO chains to diffuse out of the silicate galleries.

Experimental Section

PEO (number-average molecular weight, M_n = 4800 g/mol) was purchased from Aldrich and further purified by precipitation into *n*-hexane twice. The molecular weight distribution was 1.05, as determined by size-exclusion chromatography using tetrahydrofuran as the solvent and PS as standards. C10A was purchased from Southern Clay Products, Inc., and was used directly without further purification. The lateral particle size ranged from 0.4 to 1.0 μm, and the aspect ratio was over 200.[18] Because of this large anisotropy of the layered silicates, oriented clay particles were obtained from simple solution casting on flat surfaces. Differential scanning calorimetry (DSC) results indicated that the hydrogenated tallow (~65% C18; ~30% C16; ~5% C14) was amorphous in the temperature ranges studied. The nanocomposite was prepared by mixing C10A and PEO in chloroform with different ratios (PEO/C10A-*x*, where *x* denotes the weight percentage of C10A). We noticed that benzene and toluene did not provide good PEO intercalation, because the C10A was not fully exfoliated in these solvents, as reported by Ho et al.[18] After ultrasonication for 1 h, the solvent was evaporated in a fume hood for 3 days, followed by annealing at 50 °C for 2 days and subsequently at 90 °C for 24 h in a vacuum oven.

DSC experiments were carried out on a TA Instruments DSC-2920, which was calibrated with a standard indium sample. To avoid thermal lag, the sample weight was kept around 1.0 mg. To determine the clay content, thermogravimetric analysis was performed at a heating rate of 20 °C/min on a Perkin-Elmer TGA7 under a nitrogen atmosphere (we noted that C10A itself had a 61 wt % inorganic content).

Two-dimensional (2D) time-resolved WAXD experiments were performed at the X27C beamline in National Synchrotron Light Source, Brookhaven National Laboratory, using an imaging plate as the detector. A small lead beam stop was used to reach low angles with $q = 1.0$ nm^{-1} (d-spacing of 6.28 nm). For clarity, the total X-ray data were divided into two parts: small-angle X-ray scattering (SAXS) in the range of 1−8 nm^{-1} and WAXD in the range of 5−30 nm^{-1}. One-dimensional (1D) profiles were obtained by an integration of the corresponding 2D patterns. The wavelength of the X-ray beam was 0.137 nm. Silver behenate was used for the calibration of the beam center and scattering vector $q = 4\pi \sin\theta/\lambda$ with θ being half the scattering angle and λ being the wavelength. An Instec HCS410 hot stage with a liquid-nitrogen cooling accessory was used to heat and cool the nanocomposites during X-ray experiments.

Results and Discussion

In general, three components were present in these nanocomposites: (i) C10A particles, (ii) amorphous PEO intercalated in clay galleries, and (iii) PEO outside of clay galleries which could crystallize. For the PEO content above 85 wt %, all PEO was intercalated, and no de-intercalation was observed. On the other hand, when the PEO content was less than 15 wt %, the X-ray reflections from clay particles were not strong enough for detailed analysis. Therefore, we chose nanocomposites with a clay content of about 50 wt % for two purposes: (i) clear clay layer signals in the X-ray experiments and (ii) enough PEO outside of the clay galleries to crystallize and generate enough material depletion potential for de-intercalation processes.

The morphology of the PEO/C10A-53 nanocomposite was studied using temperature-dependent X-ray diffraction experiments. Typical 1D SAXS and WAXD profiles for PEO/C10A-53 at various temperatures are shown in Figure 1. The sample was first melted at 70 °C for 5 min followed by cooling to −30 °C and then heating to 70 °C at 0.8 °C/min. At 70 °C, the PEO in the nanocomposite was observed to be amorphous. The sample showed well-defined layer morphology with q ratios being 1:2:3:4 in the SAXS profiles in Figure 1A. Note that the reversal of the first and second-order reflection intensities originated from the Lorentz corrections to the raw data. The overall layer thickness (L) was 3.18 nm. Comparing with the layer thickness of pure C10A (~1.86 nm), the intercalated PEO layer thickness was 1.32 nm. In Figure 1B, the WAXD profile at 70 °C showed a strong reflection at q = 14.2 nm^{-1} [overlapped (110) and (020) reflections from the 2D crystals of layered silicates],[1] superposing with an amorphous halo originated from the amorphous PEO and surfactants. When the temperature decreased to 44 °C, PEO outside the silicate particles started to crystallize, as shown by the (120) and mixed (032)/($\bar{1}$32) reflections from the monoclinic PEO crystals at 13.6 and 16.6 nm^{-1}, respectively. Meanwhile, the first-order lamellar reflection became less intense and higher order peaks gradually diminished. This phenomenon could not be explained by the decrease in the electron density difference as PEO crystallizes, because PEO crystallized outside the clay particles and it did not contribute to the clay reflections. Instead, this had to be attributed to the disruption of the 1D long-range order in the clay stacking. We speculated that during the primary crystallization process the intercalated PEO chains started to be randomly "extracted" from individual clay galleries, resulting in "defects" in the 1D long-range order. However, these defects did not have enough populations to result in the observation of substantial d-spacing changes in the intercalated clay particles (see Figure 2). Intriguingly, with further decreasing the temperature, the first-order

(15) Manias, E.; Kuppa, V.; Yang, D.-K.; Zax, D. B. *Colloids Surf., A* **2001**, *187−188*, 509.
(16) Kuppa, V.; Foley, T. M. D.; Manias, E. *Eur. Phys. J. E* **2003**, *12*, 159.
(17) Harris, D. J.; Bonagamba, T. J.; Schmidt-Rohr, K. *Macromolecules* **1999**, *32*, 6718.
(18) Ho, D.; Briber, R. M.; Glinka, C. J. *Chem. Mater.* **2001**, *13*, 1923.

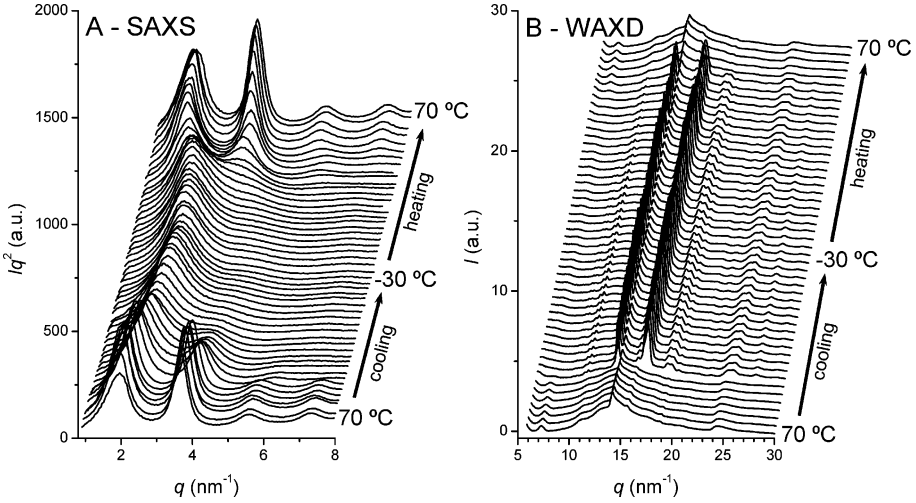

Figure 1. 1D Lorentz-corrected SAXS (A) and WAXD (B) profiles at different temperatures for the PEO/C10A-53 nanocomposite. The ramping rate was 0.8 °C/min, and each interval between neighboring curves is 4 °C.

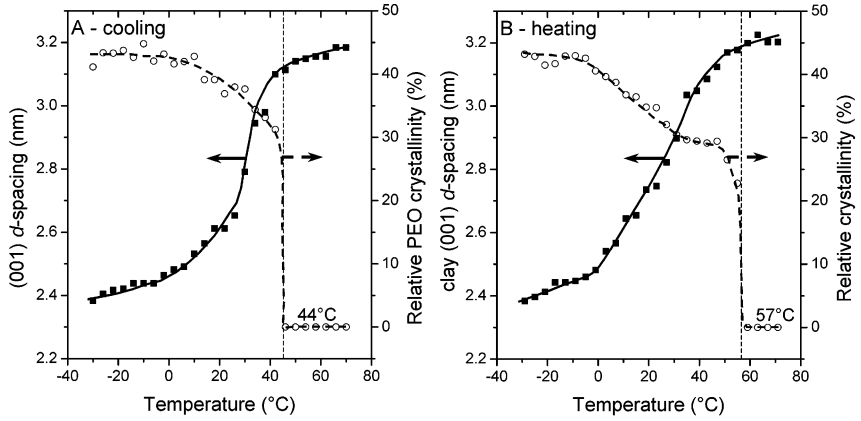

Figure 2. PEO/C10A-53 (001) *d*-spacing changes (solid squares) with temperature during (A) cooling and (B) heating processes. Corresponding relative PEO crystallinity changes with temperature are shown as open circles.

lamellar reflection gradually shifted to higher q values, indicating decreases in L (de-intercalation) due to the self-generated depletion fields from PEO crystallization outside the clay particles. During the subsequent heating process, the first-order reflection in SAXS gradually shifted back to lower q values, indicating an increase in L (i.e., interaction) due to the diffusion of PEO chains back into the silicate galleries. The corresponding WAXD profiles in Figure 1B showed a melting temperature (T_m) of 57 °C.

To quantify the reversible de-intercalation and intercalation processes observed in the PEO/C10A-53 nanocomposite and their relationship with PEO crystallization and melting, L and the relative PEO crystallinity[19] are plotted as a function of temperature in Figure 2. During the cooling process in Figure 2A, a primary PEO crystallization was seen at 44 °C; that is, the relative crystallinity jumped from 0 to ~30 wt %. However, only a slight decrease in L was observed when compared with that at 70 °C, although the primary PEO crystallization generated defects in the clay stacking as mentioned above. With a further decrease in temperature to 0 °C, the relative PEO crystallinity continuously increased to ~40 wt %, suggesting that a significant portion of PEO underwent secondary crystallization within the system. The secondary PEO crystallization was also observed in a parallel DSC study with the same scan rate of 0.8 °C/min (see Figure S1 in Supporting Information). Upon cooling from 70 °C, the normalized heat of transition for PEO primary crystallization at 44.0 °C was found to be 148.4 J/g, corresponding to a crystallinity of 78.7 wt %. The heat of fusion for the extended chain PEO (5K g/mol) crystals was 188.6 J/g.[20] Upon a subsequent heating process after the sample has been cooled to −30 °C, the normalized heat of fusion for PEO crystals (at 57.0 °C) was 166.8 J/g and the corresponding crystallinity was, thus, 88.4 wt %. The difference between the heats of transitions during the cooling and the heating processes could be attributed to the secondary PEO crystallization. This result was qualitatively consistent with the WAXD results in Figure 2.

Surprisingly, a substantial decrease in L was observed during secondary crystallization from 3.10 nm at 46 °C to 2.44 nm at −2 °C. The linear coefficient of the dimension change was more than 0.0044/K. This was more than 20 times greater than the linear coefficient of thermal expansion (α) of 2.17×10^{-4}/K, which was calculated from the coefficient of volume thermal expansion for amorphous PEO.[21] Therefore, the decrease in L could not be explained by thermal shrinkage alone. We speculated that the unexpectedly large dimensional change of L was because of the self-generated depletion field by the PEO secondary crystallization outside the silicate particles. In other words, to maximize the PEO crystallinity (or lower total free

(19) It is defined as the ratio of PEO crystalline peaks to the overall scattering, which also includes the C10A reflections.

(20) Sun, L.; Liu, Y.; Zhu, L.; Hsiao, B. S.; Avila-Orta, C. A. *Polymer* **2004**, *45*, 8181.

(21) McGowan, J. C. *Polymer* **1969**, *10*, 841.

energy of the system) the intercalated PEO had to diffuse out of the silicate galleries to facilitate the crystallization process taking place outside the gallery.

During the subsequent heating process, the poor crystals formed by secondary crystallization started to melt around 0 °C (Figure 2B), slightly above the temperature where the secondary crystallization started to level off upon cooling in Figure 2A. This was consistent with recent fast DSC studies showing that poor crystals melted at temperatures only slightly higher than the crystallization temperature.[22] At the same time, the L value was found to increase upon heating. This increase appeared to be linear until leveling off at temperatures above 50 °C. The melting of PEO crystals formed in primary crystallization occurred at 57 °C, evidenced by a relative PEO crystallinity drop from 30 to 0 wt %. Again, there was no substantial change in the L value during the melting process of primary PEO crystals outside the silicate galleries.

The above experimental observations suggested that de-intercalation was induced by PEO secondary crystallization and intercalation happened after subsequent melting of secondary PEO crystals. The subsequent intercalation could be attributed to the favorable interaction of PEO with the organic surfaces of layered silicates to reach an equilibrium gallery thickness (3.18 nm in this case).[24] However, it is still unclear where the secondary crystallization takes place and why it is such an effective way to drive the PEO chains out of the silicate galleries. To answer these questions, the morphology of the nanocomposite needs to be understood. 2D WAXD patterns of the PEO/C10A-53 nanocomposite before (70 °C) and after (22 °C) PEO crystallization are shown in Figure 3. The orientations of organically modified silicates and PEO lamellar crystals can be obtained from the azimuthal profiles shown in Figure 3C. For the WAXD pattern at 70 °C, the silicate layer reflections were seen on the meridian, indicating that they were aligned horizontally. When the temperature decreases to 22 °C, the PEO chains outside the primary silicate particles began to crystallize. However, our SAXS profile, reaching to even lower q values, showed no PEO crystalline lamellar reflections (see Figure S2 in Supporting Information). On the basis of the transmission electron microscopy (TEM) observations (see Figure S3 in Supporting Information), the primary silicate particles were uniformly dispersed in the matrix, and we speculated that PEO crystals did not have enough space to stack together to form multiple layers. From the azimuthal scan profiles in Figure 3C, the layered silicates exhibited two (002) reflections at 90 and 269°, indicating again a horizontal orientation of the silicate layers. The PEO (120) reflections exhibited two maxima at −2 and 176°, suggesting that the PEO chains were vertically aligned. The mixed PEO (032)/($\bar{1}$32) reflections showed four maxima at 33, 155, 220, and 320°, respectively. This is similar to the PEO fiber pattern with the fiber axis in the meridian direction.[23] These results suggest that the PEO lamellae are oriented horizontally, and a schematic representation of the PEO/C10A nanocomposite is shown in Figure 4.

In this schematic diagram, an interphase PEO layer exists, which was between the silicate particles and the PEO lamellar crystals. As a result of the large surface

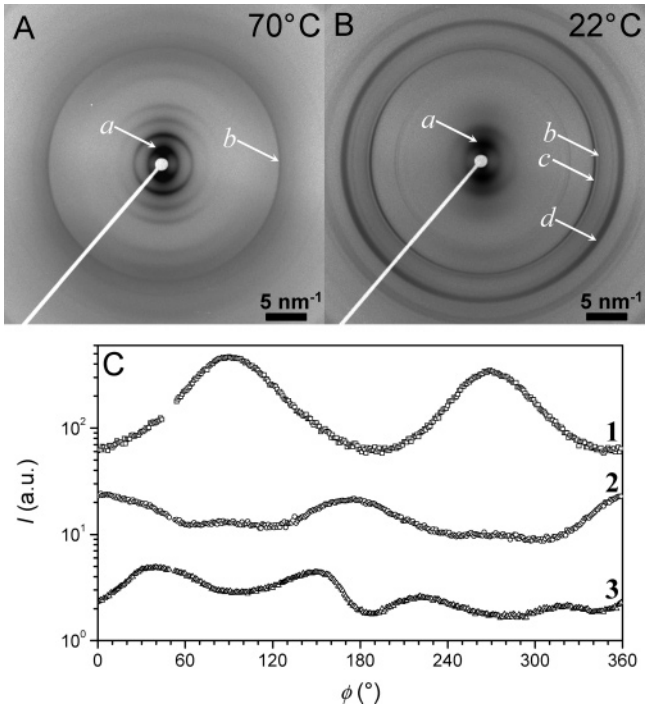

Figure 3. 2D WAXD patterns of PEO/C10A-50 nanocomposite at (A) 70 and (B) 22 °C: (a) silicate (001) reflection; (b) overlapped silicate (110) and (020) reflections; (c) PEO (120) reflection; and (d) mixed PEO (032)/($\bar{1}$32) reflections. The intensities are in logarithmic scales. The azimuthal scan results from the patterns in part B are shown in part C for the (1) silicate (002) reflection; (2) PEO (120) reflection; and (3) mixed PEO (032)/($\bar{1}$32) reflections.

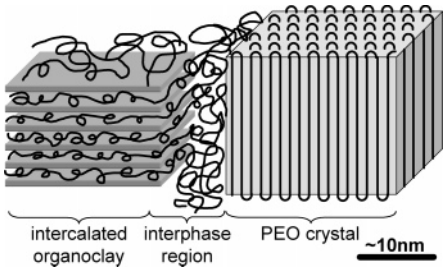

Figure 4. Schematic representation of the morphology in the PEO/C10A-53 nanocomposite after PEO primary crystallization.

area of the inorganic nanofiller, the properties of these interphases may differ dramatically from those of the bulk polymer.[3] It is speculated that this interphase layer has a finite size and the secondary PEO crystallization may take place in these interphases. Presumably, the secondary PEO crystals are surface-nucleated on the existing PEO crystal surfaces. During secondary PEO crystallization, the intercalated amorphous PEO can gradually diffuse out as a result of a crystallization-generated depletion field.

Conclusions

Reversible de-intercalation and intercalation were observed in PEO/C10A nanocomposites, which we suggested were induced by secondary PEO crystallization and subsequent melting of secondary PEO crystals outside of the clay galleries. On the basis of the 2D WAXD results, an interphase layer between the silicate primary particles and the PEO lamellar crystals was proposed. In this model, secondary PEO crystallization within these interphases was responsible for the diffusion of amorphous PEO chains

(22) Minakov, A. A.; Mordvintsev, D. A.; Schick, C. *Polymer* **2004**, *45*, 3755.
(23) Zhu, L.; Cheng, S. Z. D.; Calhoun, B. H.; Ge, Q.; Quirk, R. P.; Thomas, E. L.; Hsiao, B. S.; Yeh, F.; Lotz, B. *J. Am. Chem. Soc.* **2000**, *122*, 5957.
(24) Giannelis, E. P.; Krishnamoorti, R.; Manias, E. *Adv. Polym. Sci.* **1999**, *138*, 107.

out of the silicate galleries. This pathway might enable the investigation of pure polymer chain diffusion within the silicate gallery without the interference of polymer chain diffusion from the bulk into silicate primary particles. A study on the PEO diffusion rate within the silicate gallery is currently underway.

Acknowledgment. This work was supported by the startup funds provided by The University of Connecticut, the ACS Petroleum Research Fund (41918-G7), and a NSF CAREER award (DMR-0348724). The synchrotron X-ray experiments were carried out in the National Synchrotron Light Source, Brookhaven National Laboratory, which is supported by the Department of Energy Grant DE-FG02-99ER 45760.

Supporting Information Available: DSC study on PEO secondary crystallization, effect of organoclay content on the PEO crystalline lamellar morphology studied by SAXS, and dispersion of organoclay in the PEO matrix studied by TEM. This material is available free of charge via the Internet at http://pubs.acs.org.

LA047087C